*Transactions*, SMiRT-24
BEXCO, Busan, Korea - August 20-25, 2017
Division VI

# STATIC LOADING TEST ON SEISIMIC CAPACITY OF REINFORCED CONCRETE SHEAR WALLS IN NUCLEAR POWER PLANT Part 2 EVALUATION OF DAMAGE AND RESIDUAL CAPACITY

**Masaki Maeda[1], Norihiro Hosoya[2], Takuya Koike[3], Mamoru Hanzawa[2], Yoshihiro Ogata[4], Kiwoong Jin[5]**

[1] Professor, Department of Architecture and Building Science, Tohoku University, Japan
[2] Graduate Student, Department of Architecture and Building Science, Tohoku University, Japan
[3] Structural Engineer, Suzuki Architectural Design Office, Japan
[4] Manager, Civil & Architectural Engineering Dept., Tohoku Electric Power Co.,Inc. , Japan
[5] Assistant Professor, Department of Architecture and Building Science, Tohoku University, Japan

## ABSTRACT

The maximum earthquake response in No.2 Reactor Building in Onagawa nuclear power plant of Tohoku Electric Power Company, Japan, was reported to remain within an elastic state based on damage survey and simulation after the 2011 Great East Japan Earthquake. However, minor cracks were observed in shear walls in the building and stiffness degradation was predicted by accelerometer records during the earthquake. The non-linear behaviour including stiffness degradation after cracking has not been strongly focused on the seismic design and performance evaluation practice of reactor buildings in Japan, because such remarkable stiffness degradation has not been found previously. Therefore, in order to develop more accurate evaluation methodology of seismic performance for a reactor building, it is necessary to investigate the effect of cracking in shear walls on their seismic capacity.

In this paper (Part. 2), therefore, static loading tests of shear walls are conducted. The reinforcement ratio and damage levels was employed as major parameters for the specimens. Different levels of damage were induced to specimens by “pre-loading”, and the result were compared with no-pre-damaged specimen. Degradation in ultimate strength, ductility and energy dissipation capacity of damaged shear walls are selected as major indicators for residual seismic capacity.

From the experiment result, it was found that the damage level in a shear wall does not strongly influence the seismic performance at the ultimate state, such as ultimate shear strength, deformation and energy dissipation capacities, in spite of the stiffness degradation within the range of earthquake response experienced in pre-loading.

## INTRODUCTION

The purpose of this paper is to investigate the influence of pre-damage levels and reinforcement ratio on the ultimate state performances, such as shear strength, deformation and energy dissipation capacity by conducting static cycle loading tests of reinforced concrete shear walls.

## EXPERIMENTAL PLAN

### *Outline of experiment*

The experimental program consists of nine reinforced concrete shear wall specimens. The shear wall was designed to be shear critical walls in about 1/4 scale of prototype reactor building in a nuclear

power plant. The test parameters are different damage levels induced to each specimen (S-DI, II, III, IV) by pre-loading and different reinforcement ratio (1.32% or 0.66%), as shown in **Table 1**. Specimens S-13-D0 and S-06-D0 are tested without pre-loading to investigate capacity of the original shear walls. Note that specimens S-13-DII and S-06-DII were re-used as specimens S-13-DIV and S-06-DIV. In other words, at first these specimens were treated as S-13-DII and S-06-DII, and pre-loadings were conducted until the damage level II, then the main-loadings were conducted until damage level IV, which were also considered as pre-loading for S-13-DIV and S-06-DIV. After that, the main-loading for specimens S-13-DIV and S-06-DIV was carried out. This is because the pre-damage level Ⅱ was considered to be quite limited and minor, and the capacity deterioration due to the first time of pre-loading was regarded as negligible.

**Table 1** Summary of specimens

| | Name of specimen | S-13 series | | | | | S-06 series | | | |
|---|---|---|---|---|---|---|---|---|---|---|
| | | S-13-D0 | S-13-DI | S-13-DII | S-13-DIII | S-13-DIV | S-06-D0 | S-06-DII | S-06-DIII | S-06-DIV |
| Parameter | **(1) Damage class** | **0** | **I** | **II** | **III** | **IV** | **0** | **II** | **III** | **IV** |
| | **(2)Reinforcement ratio *Ps* (%)** | **1.32** | | | | | **0.66** | | | |
| Shear wall | Height (mm) | 1000 | | | | | | | | |
| | Length (mm) | 1800 | | | | | | | | |
| | Thickness (mm) | 120 | | | | | | | | |
| | **Arrangement of reinforcement** | **D6@40(SD295) Double** | | | | | **D6@80(SD295) Double** | | | |
| | Axial stress (MPa) | 0.50 | | | | | | | | |
| | Shear span to depth ratio (MPa) | 0.29 | | | | | | | | |
| Column | Section b×D (mm) | 200×200 | | | | | | | | |
| | Main reinforcement | 12-D16(SD345) | | | | | | | | |
| | Hoop reinforcement | 2-D10(SD345) @60 | | | | | | | | |
| Beam | Section b×D (mm) | 400×400 | | | | | | | | |
| | Main reinforcement | 10-D22(SD390) | | | | | | | | |
| | Hoop reinforcement | 2-D13(SD390)@100 | | | | | | | | |
| Shear cracking strength by AIJ[2] (kN) | | 326 | | | | | 301 | | | |
| Ultimate shear strength by AIJ[2] (kN) | | 1499 | | | | | 1370 | | | |
| Ultimate shear strength by AIJ [3] (kN) | | 915 | | | | | 739 | | | |
| Crack flexural strength by AIJ[3] (kN) | | 647 | | | | | 599 | | | |
| Ultimate flexural strength by AIJ[3] (kN) | | 2802 | | | | | 2452 | | | |

The strength shown in **Table 1** were calculated by current design guidelines [2, 3]. Two design equations were employed for prediction of the ultimate shear strength; one is AIJ (Architectural Institute of Japan) design guideline based on the truss and arch theory (Eq. (1)) [2], and another is JEAC's guideline [4]. The deformation at each damage level was decided from the experimental results of specimen S-13-D0 and S-06-D0. According to the determined damage levels, the pre-loadings for S-13-DI~IV and S-06-DI~IV were conducted.

$$V_u = t_w l_{wb} P_s \sigma_{sy} \cot\phi + \tan\theta(1-\beta) t_w l_{wa} \nu\sigma_B / 2 \qquad (1)$$
$$\beta = \{(1+\cot^2\phi) P_s \sigma_{sy}\} / \nu\sigma_B, \quad \tan\theta = \sqrt{(h_w / l_{wa})^2 + 1} - h_w / l_{wa}$$

Where, $t_w$: Wall thickness (mm), $l_{wa}$, $l_{wb}$: Equivalent wall length(mm),
$P_s$ : Shear reinforcement ratio of the wall, $v$ : Effective compression strength coefficient,
$\sigma_{sy}$ : Strength of the shear reinforcement of the wall, $\sigma_B$ : Compressive strength of concrete,
$\phi$ : Angle of concrete compression strut of truss mechanism
$h_w$: Wall height(mm)

### *Outline of specimen*

The reinforcement arrangement is shown in **Figure 1**. All specimens have two columns in both sides of a wall panel, and top and base beams. The height of a specimen is 1800mm, and the wall panel is 1000mm height and 120mm thickness. The reinforcement detail of S-13 series specimens was decided to be 2-D6@40, at the same time, the reinforcement ratio of S-06 series specimens is half of S-13 series specimens and their reinforcement detail was decided to be 2-D6@80.

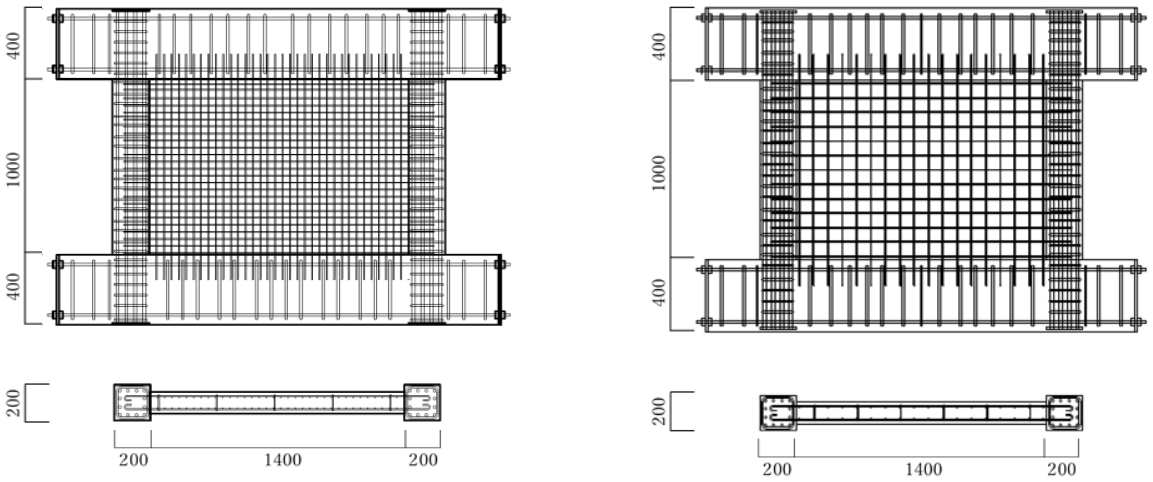


(a) S-13 series (b) S-06 series

**Figure 1** Reinforcing detail of specimen: elevation and section

### *Loading plan*

**Figure 2** shows the loading test setup. Vertical loads were applied uniformly on the total cross-section of the wall and columns by two vertical hydraulic jacks and constant axial stress is about 0.5MPa. Cyclic horizontal loads were applied by two hydraulic jacks fixed at the mid-height of the wall panel so that the inflection point can develop at the same height. As a result, shear span ratio of the wall specimens is about 1/4. As shown in **Figure 3**, a pre-loading was applied to the specimens, except no-pre-damaged specimens S-13-D0 and S-06-D0, in order to simulate the damage state of shear walls after suffering the earthquake. After that, the main-loading was applied to all specimens. As mentioned above, whether the damage level after the earthquake affects the subsequent structure performance degradation will be compared and investigated from the test results.

**Table 2** shows the loading cycle. The loading cycle for no-pre-damaged specimen S-13-D0 and S-06-D0 consists of two cycles at each story drift angle. Based on the test results of these specimens, the maximum drift of the pre-loading for each damage level is decided. The maximum drift angles in pre-loadings correspond to the target damage levels: slight, minor, moderate and severe. After five cycles of

loading at the target damage level, the specimen was unloaded by gradually reduced cyclic loading and the main-loading was conducted.

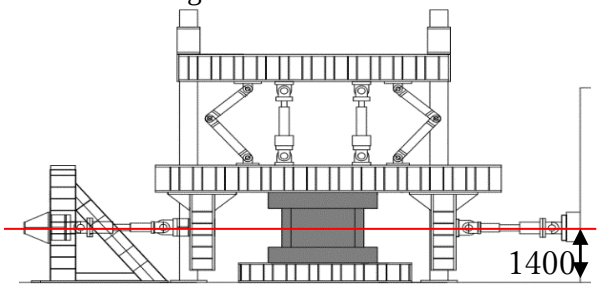


**Figure 2** Loading test setup

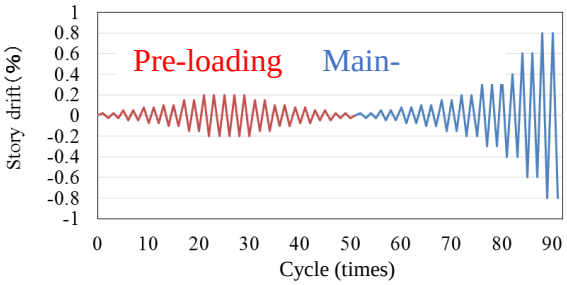


**Figure 3** Loading history

**Table 2** Loading cycle: S-13-D0 and S-06-D0

(a) S-13-D0 (no pre-damage, *Ps*=1.32%)

| Loading type | Specimens | Story Drift R(/1000rad.) and Number of Each Cycle (Time) | | | | | | | | | | | | | |
|---|---|---|---|---|---|---|---|---|---|---|---|---|---|---|---|
| | | ±0.25 | ±0.5 | ±0.75 | ±1 | ±2 | ±3 | ±4 | ±6 | ±4 | ±3 | ±2 | ±1 | ±0.5 | ±0.25 |
| Pre | S-13-D0 | None | | | | | | | | | | | | | |
| Loading type | Specimens | Story Drift R(/1000rad.) and Number of Each Cycle (Time) | | | | | | | | | | | | | |
| | | ±0.25 | ±0.5 | ±0.75 | ±1 | ±1.5 | ±2 | ±2.5 | ±3 | ±4 | ±6 | ±7 | 8 | | |
| Main | S-13-D0 | 2 | 2 | 2 | 2 | 2 | 2 | 2 | 2 | 2 | 2 | 2 | 2 | | |

(b) S-06-D0 (no pre-damage, *Ps*=0.66%)

| Loading type | Specimens | Story Drift R(/1000rad.) and Number of Each Cycle (Time) | | | | | | | | | | | | | |
|---|---|---|---|---|---|---|---|---|---|---|---|---|---|---|---|
| | | ±0.25 | ±0.5 | ±0.75 | ±1 | ±2 | ±3 | ±4 | ±6 | ±4 | ±3 | ±2 | ±1 | ±0.5 | ±0.25 |
| Pre | S-06-D0 | None | | | | | | | | | | | | | |
| Loading type | Specimens | Story Drift R(/1000rad.) and Number of Each Cycle (Time) | | | | | | | | | | | | | |
| | | ±0.25 | ±0.5 | ±0.75 | ±1 | ±2 | ±3 | ±4 | ±6 | 8 | | | | | |
| Main | S-06-D0 | 2 | 2 | 2 | 2 | 2 | 2 | 2 | 2 | 2 | | | | | |

## EXPERIMENTAL RESULTS OF THE EXPERIMENT: S-D0

### *Shear force-displacement relationship and failure behavior of specimen S-13-D0 and S-06-D0 without pre-damage*

The shear force-story drift angle relationship of specimens S-13-D0 and S-06-D0 is shown in **Figure 4** associated with a back bone curve calculated by JEAC design guideline [4]. In addition, crack patterns and final damage states are shown in **Figure 5**. Note that the damage check was carried out only in the left side of the specimen during the loading test, because symmetrical stress distribution and damage patterns were predicted in the left and the right side.

Initial cracks in both specimens were observed at the corner of the wall panel at a cycle of 0.25/1000rad. At the cycle of 2/1000rad., cracks developed in the entire wall panel. After that, in specimen S-13-D0, the crack interval was found to be close to the value of reinforcement interval. Furthermore, the vertical reinforcement of the column and wall panel yielded at 5/1000rad., and the horizontal reinforcement of the wall panel yielded at 6/1000rad. In addition, after slight concrete spalling was observed at the corner of the wall panel at the same cycle, the shear force reached the maximum. After that, the concrete spalling and rapid drop in shear force occurred at 8/1000rad.

On the other hand, in the case of S-06-D0 in which the reinforcement ratio (*Ps*=0.66%) is half of S-13-D0, the yield point of the vertical reinforcement and horizontal reinforcement was observed at 3/1000rad. and 4/1000rad., respectively. At 6/1000rad., the shear force reached the maximum with

concrete spalling, and then rapid shear strength drop began.

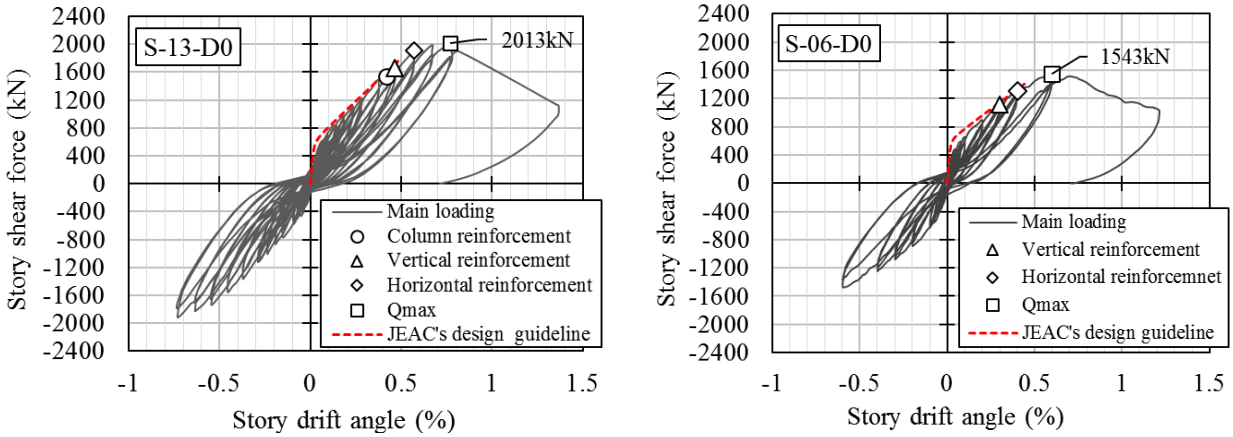


(a) S-13-D0 (b) S-06-D0

**Figure 4** Shear force-story drift angle relationship of S-13-D0 and S-06-D0

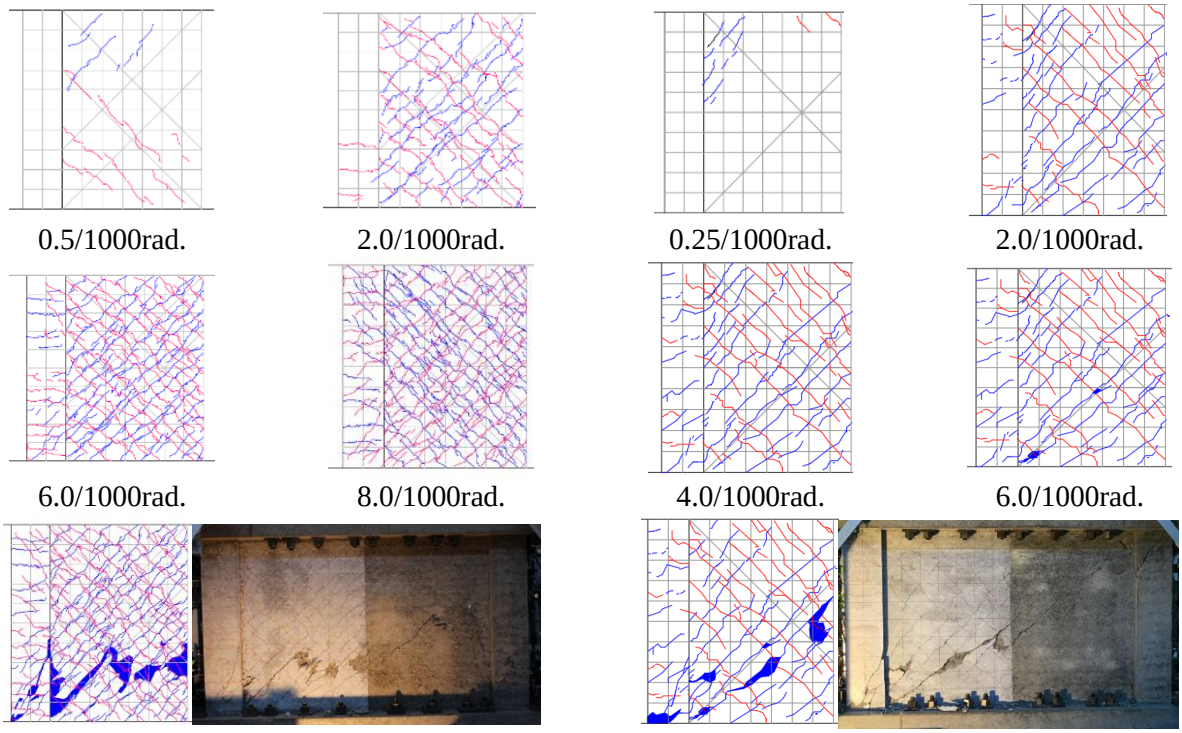


ultimate stage ultimate stage

(a) S-13-D0 (b) S-06-D0

**Figure 5** Cracking patterns of S-13-D0 and S-06-D0

***Classification of damage class in specimen S-13-D0 and S-06-D0***

In Japan, Post-earthquake Damage Evaluation Guideline, originally issued in 1990, was revised in 2001 and 2015 [5]. In the Guideline, damage classes of structural elements are classified into five classes according to **Table 3** and **Figure 6**, based on the damage situation such as the residual crack width, spalling of concrete, and buckling or fracture of steel bars.

**Table 3** Damage classes of structural elements from Japanese damage evaluation guideline [5]

| Damage class | Damage situation |
|---|---|
| Ⅰ | Some cracks are found. Crack width is smaller than 0.2 mm. |
| Ⅱ | Cracks of 0.2 - 1 mm wide are found. |
| Ⅲ | Heavy cracks of 1 - 2 mm wide are found. Some spalling of concrete is observed. |
| Ⅳ | Many heavy cracks are found. Crack width is larger than 2 mm. Reinforcing bars are exposed due to spalling of the cover concrete. |
| Ⅴ | Buckling of reinforcement, crushing of concrete and vertical deformation of columns and/or shear walls are found. Side-sway, subsidence of upper floors, and/or fracture of reinforcing bars are observed in some cases. |

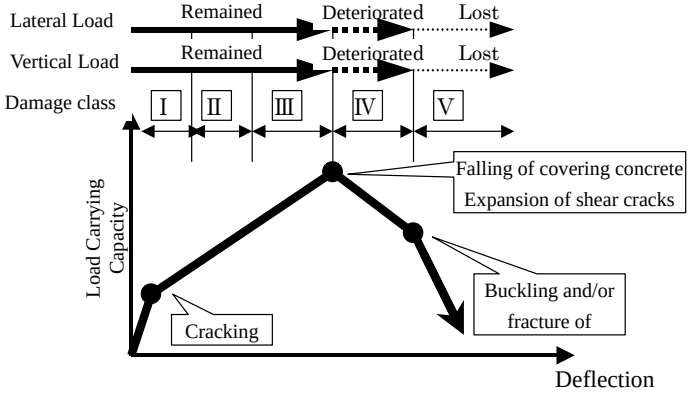


**Figure 6** Idealized lateral force-displacement relationship and damage class[2]

In this paper, damage classes in the shear walls (S-13-D0 and S-06-D0) are judged based on the Post-Earthquake Damage Evaluation Guideline. Also, the load-deflection curve, stiffness degrading ratio and yielding states of the reinforcement, which are shown in **Figure 7**, as well as the crack width/length, are considered to determine those damage classes and their corresponding story drift. As a result, the damage class I corresponding to the cracking drift is found less than 1/1000rad, the drift of 1/1000rad~3/1000rad is for damage class II, the drift of 3/1000rad~5/1000rad is for damage class III, and the drift of 5/1000rad~ultimate shear strength is determined as the damage class IV. Thus, pre-loadings for specimens S-DI~IV were carried out, as shown in **Table 4**.

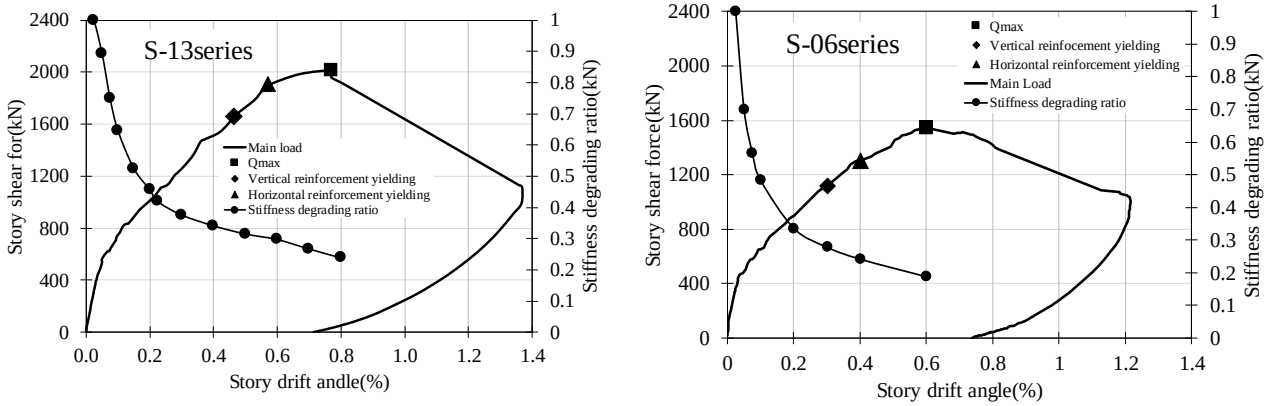

**Figure 7** Load-deflection envelope and stiffness degrading ratio

**Table 4** Loading cycle of pre-damaged specimens: S-13-DI~ DIV and S-06-DI~DIV

| Loading type | Specimens | Story Drift R(/1000rad.) and Number of Each Cycle | | | | | | | | | | | | | |
|---|---|---|---|---|---|---|---|---|---|---|---|---|---|---|---|
| | | ±0.25 | ±0.5 | ±0.75 | ±1 | ±2 | ±3 | ±4 | ±6 | ±4 | ±3 | ±2 | ±1 | ±0.5 | ±0.25 |
| Pre | S-13-DI | 2 | 2 | 5 | | | | | | | | | | 2 | 2 |
| | S-13-DII | 2 | 2 | 2 | 2 | 5 | | | | | | | 2 | 2 | 2 |
| | S-13-DIII | 2 | 2 | 2 | 2 | 2 | 2 | 5 | | 2 | 2 | 2 | 2 | 2 | 2 |
| | S-13-DIV | 2 | 2 | 2 | 2 | 2 | 2 | 2 | 5 | 2 | 2 | 2 | 2 | 2 | 2 |
| | S-06-DII | 2 | 2 | 2 | 2 | 5 | | | | | | | 2 | 2 | 2 |
| | S-06-DIII | 2 | 2 | 2 | 2 | 2 | 2 | 5 | | 2 | 2 | 2 | 2 | 2 | 2 |
| | S-06-DIV | 2 | 2 | 2 | 2 | 2 | 2 | 2 | 5 | 2 | 2 | 2 | 2 | 2 | 2 |

| Loading type | Specimens | Story Drift R(/1000rad.) and Number of Each Cycle | | | | | | | | | | | |
|---|---|---|---|---|---|---|---|---|---|---|---|---|---|
| | | ±0.25 | ±0.5 | ±0.75 | ±1 | ±1.5 | ±2 | ±2.5 | ±3 | ±4 | ±6 | ±7 | 8 |
| Main | All | 2 | 2 | 2 | 2 | 2 | 2 | 2 | 2 | 2 | 2 | 2 | 2 |

## EXPERIMENTAL RESULTS OF DAMEGED SPECIMENS: S-13-DI~ DIV AND S-06-DI~DIV

### *Shear force-story drift angle relationship of damaged specimens*

The shear force-story drift angle relationship of specimens S-13-DI~IV and S-06-DI~IV is shown in **Figure 8**. In S-13 series, development of damage in all of the specimens respectively indicate similar trend with un-damaged specimens S-13-D0 and S-06-D0, cracks developed from the wall corners, reinforcement yielded at 6/1000rad., 4/1000rad. In S-13 series, all of the specimen reached the maximum shear force at 8/1000rad. On the other hand, in S-06 series, all of the specimens reached the maximum shear force at 6/1000rad, except S-06-DIV, which reached the maximum shear force at the next cycle of 8/1000rad.

Furthermore, the ultimate damage stage of each specimen is shown in **Figure 9**. Regardless of reinforcement ratio, almost all specimens with pre-damage of 0, I, II and III reached their ultimate stages with concrete spalling of the column and wall panel. On the other hand, only the specimen S-06-DIV reached its ultimate stage with concrete spalling of the wall panel. This is because shear strength of the wall panel degraded due to severe damage induced by pre-loading, and these results indicate that the damage at the ultimate stage may be influenced by the previous earthquake damage, if the wall has relatively low reinforcement ratio.

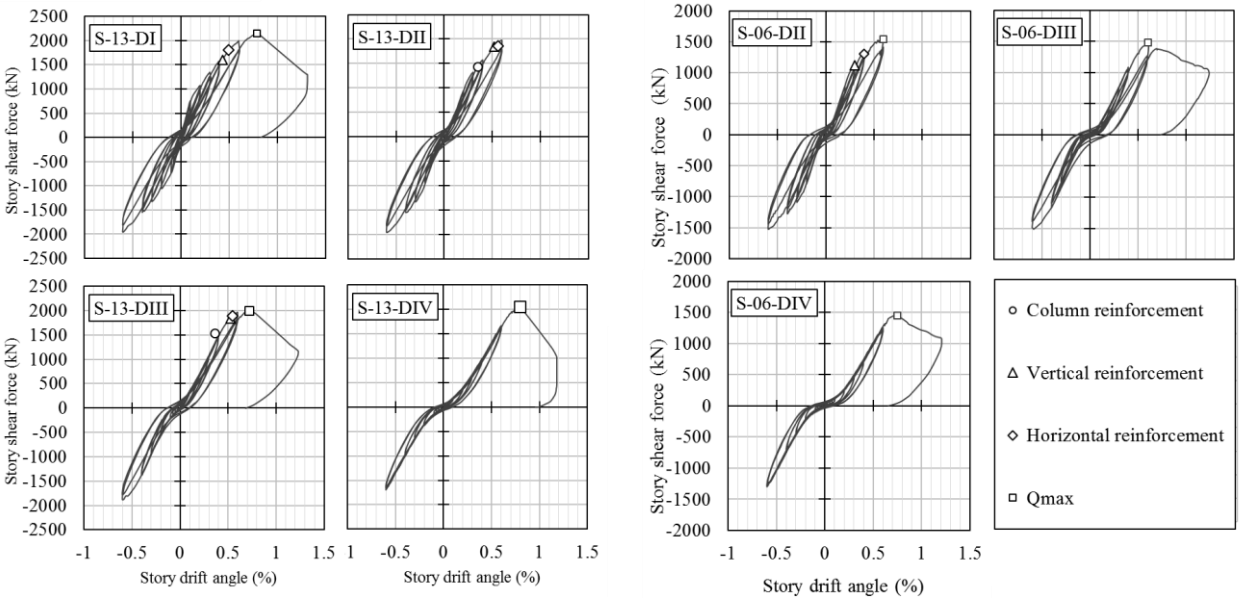

(a) S-13 series (b) S-06 series

**Figure 8** Shear force-story drift angle relationship of specimens S-13-DI~IV and S-06-DI~IV

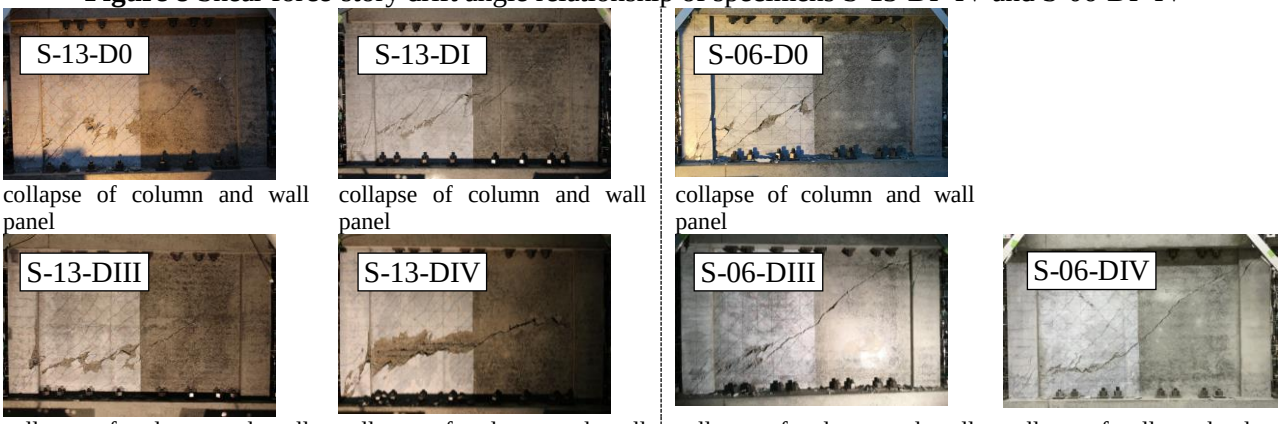


(a) S-13 series (b) S-06 series

**Figure 9** The damage state at ultimate stage

## Influence of reinforcement ratio on structural performance

### *Comparison of shear strength and deformation capacity*

Envelope curves of shear force-story drift angle relationship for all specimens are shown in **Figure 10 (a)**. The story shear force ratio is shown in **Figure 10 (b)**, where the story shear force ratio is defined as the ratio of shear force at each main loading drift in the pre-damaged to the no-pre-damaged specimen. In the region within the maximum deformation during the pre-loading, the shear forces of pre-damaged specimens decreased due to the degradation of equivalent stiffness, as shown in **Figure 10**. In S-13 series, the maximum shear force of each specimen has almost no difference regardless of the damage level given by pre-loading (**Figure 10 (b)**). On the other hand, in S-06 series, comparing with the specimen S-06-D0, the maximum shear force of the specimens with damage level III or IV at their main loadings became lower. For specimens S-06-DIII and S-06-DIV, the maximum shear force degraded by 5%, 20%, respectively.

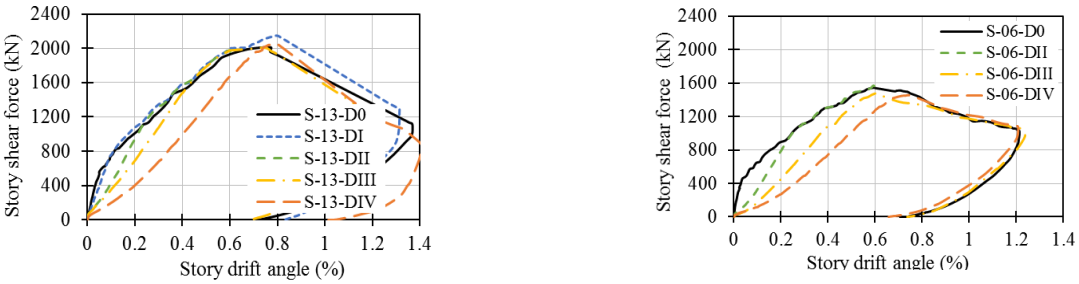


(a) Shear force-story drift envelops with different pre-damage levels

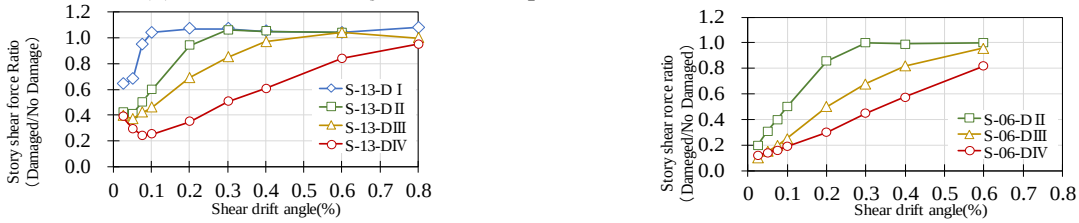


S-13 series S-06 series

(b) Comparison of story shear force ratio in each main drift angle

Fig.10 Shear force-story drift envelop and story shear force ratio in each main drift angle

***Strain distribution in wall reinforcement***

Strain distribution in wall reinforcement at the cycle of 6/1000rad. is shown in **Figure 11**. Strain gages were attached on horizontal and vertical reinforcement in the left half of the wall panel at regular intervals: 0mm, 240mm, 480mm, and 720mm from the center of the wall panel. **Figure 11** also shows the comparison of strain distribution in vertical reinforcement. The red broken line in **Figure 10** is the yield strain of reinforcement obtained by the material test. The strain distribution in vertical reinforcement has the following characteristics: 1) in S-13 series, the strain increased as a whole; 2) in S-06 series, the strain increased at the locations marked by a red box in **Figure 11**, which are in the direction of 45 degrees from the corner of the wall panel. Therefore, from the strain distribution, it is found that compression strut formed in narrow area in the S-06 series specimens due to their lower reinforcement ratio.

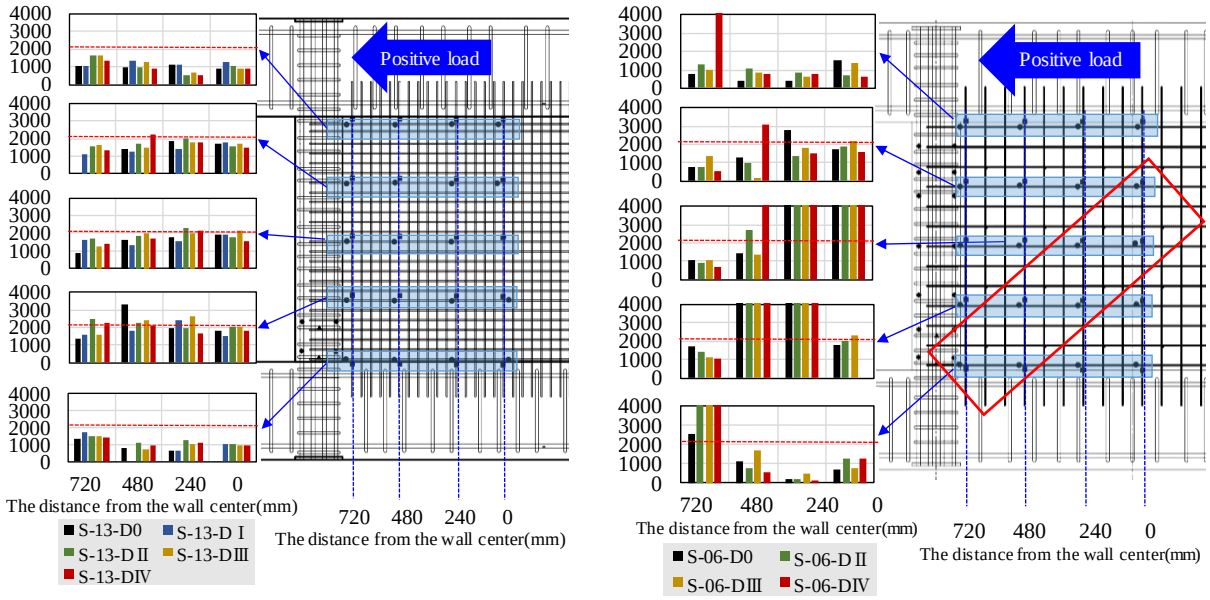


S-13 series S-06 series

**Figure 11** Strain distribution in wall reinforcement

***Comparison of energy dissipation capacity***

Energy absorption of one cycle is indicated by the loop area. Between pre-damaged and no pre-damaged specimens, the degradation of energy absorption capacity by loop area ratio, defined by Eq. (2), is compared, in order to consider the influence of damage level on energy dissipation capacity.

$$Loop\ area\ ratio = \frac{loop\ area\ of\ damaged\ specimen}{loop\ area\ of\ undamaged\ specimen} \quad \cdots\cdots(2)$$

The changes of loop area ratio is shown in **Figure 12**. In S-13 series and S-06 series, at the small story drift angle, the energy absorbing capacity of pre-damaged specimens was degraded by 40~80% according to the damage levels. However, when the story drift of the wall is in unexperienced area, the energy dissipation capacity of pre-damaged specimens in S-13 series is equal to that of no-pre-damaged one, that is, the loop area ratio is nearly equal to 1.0. On the other hand, in S-06 series, higher the damage level is, lower the energy dissipation capacity of damaged specimens becomes; that of specimen S-06-DIII degraded by 10% at the main loading of 0.6%.

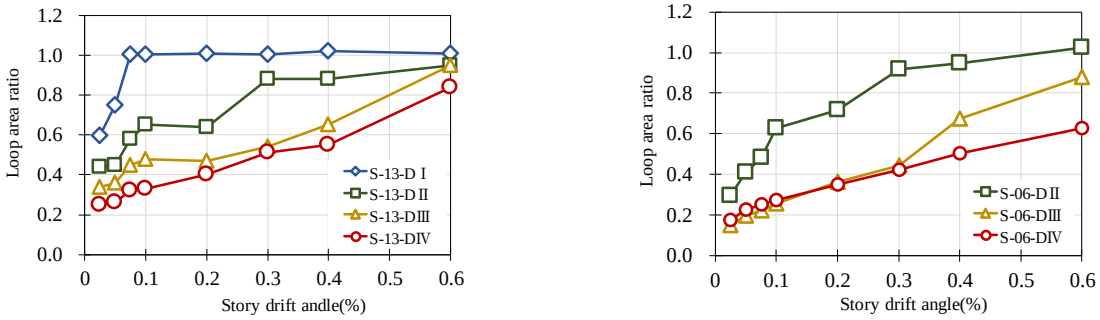


S-13 series S-06 series

**Figure 12** The changes of loop area ratio

## CONCLUSION

From experiment result, pre-damage level of the shear wall do not strongly influence the shear strength at the ultimate state. However, in the region having pre-loadings, the equivalent stiffness decreased due to the shear force degradation.

In addition, from the strain distribution, the compression strut was likely to form in a narrow area, when the wall reinforcement ratio is lower.

The energy dissipation capacity of the pre-damaged specimen degraded at the experienced story drift. However, in unexperienced area, the damage level does not strongly influence the energy absorbing capacity.

## ACKNOWLEDGEMENT

This experiment was conducted as cooperative research between Tohoku Electric Power Co. and Tohoku University. The authors would like to express great gratitude to Tohoku Electric Power Co..

## REFERENCES

Kiyoshi Hirotani et al. (2012). “Simulation Analysis of Earthquake Response of Onagawa Nuclear Power Plant to the 2011 off the Pacific Coast of Tohoku Earthquake”, *15World Conference on Earthquake Engneering*

Architectural Institute of Japan (AIJ). (1999). “Design Guidelines for Earthquake Resistant Reinforced Concrete Building Based Inelastic Displacement Concept”

Architectural Institute of Japan (AIJ). (2010). “AIJ Standard for Structural Calculation of Reinforced Concrete Structures”

Nuclear Standards Committee. “Technical Code for Seismic Design of Nuclear Power Plants”, JEAC4601-2008

Japan Building Disaster Prevention Association (JBDPA). (2001). “Standard for Post-Earthquake Damage Level Classification of Reinforced Concrete Building”